

BULK NANOCOMPOSITE RE-TM-M PERMANENT MAGNETS

M. Marinescu^{a,b*}, P. C. Pawlik^{a,b}, H. A. Davies^a, H. Chiriac^b

^aDepartment of Engineering Materials, Centre for Advanced Magnetic Materials and Devices, University of Sheffield, Mappin Street, Sheffield S1 3JD, UK

^bNational Institute of R&D for Technical Physics, 47 Mangeron Blvd. 700050 Iasi, Romania

^cInstitute of Physics, Technical University, Czestochowa, 42-200 Poland

(Pr,Dy)_xFe_{70-x}Co₁₀B₂₀ (x=4,5) bulk nanocomposite permanent magnets in the form of rods, of diameter 0.5 mm, and tubes, of outer diameter 3 mm and wall thickness up to 0.3 mm, have been prepared by devitrification annealing of amorphous precursors produced by suction die casting. The best magnetic properties were achieved for Pr₃Dy₁Fe₆₆Co₁₀B₂₀ rod and tube heat treated at 670 °C for 10min, as follows: $iH_c = 287$ kA/m, $\mu_0M_r = 0.92$ T, $(BH)_{max} = 58$ kJ/m³ and $iH_c = 293$ kA/m, $\mu_0M_r = 1.0$ T, $(BH)_{max} = 66$ kJ/m³ respectively. The bulk samples are compared in terms of their thermal stability and magnetic properties with thick ribbons of the same compositions.

(Received April 26, 2004; accepted June 3, 2004)

Keywords: Bulk nanocomposite, RE-TM-B permanent magnets, Thermal stability

1. Introduction

The good permanent magnetic properties of RE-TM-M nanocomposite alloys are generated through the magnetic hardening of the iron-based soft magnetic phase (or phases) by the RE₂TM₁₄B hard magnetic phase. This occurs when the structure is homogeneous and refined to the nanometer scale, thus ensuring effective magnetic coupling of the grains over short distances through exchange interactions. Micromagnetic modelling demonstrates the necessity for reducing the grain size to about double the domain wall width of the hard magnetic phase [1]. In practice, good magnetic properties are achieved for a crystalline structure refined to about 20nm.

Two different approaches can be adopted for the fabrication of bulk nanocomposite RE-TM-B permanent magnets: (1) the powder processing route, whereby nanostructured crushed melt spun and annealed ribbon particles are consolidated by moulding with a polymer or other binder or, more recently, (2) the devitrification annealing of amorphous bulk precursors [2], both rod and tube shaped, which yields fully dense, tablet- or ring-shaped magnets, respectively. The second approach is clearly more direct and avoids the dilution of the magnetic phase by polymer and the consequent reduction in remanence and maximum energy density. In this case, there is a challenge related to the compositional design that ensures a sufficiently high glass-forming ability (GFA) for casting to rod. The first results regarding the preparation of thick nanocomposite ribbons (thickness as high as 250µm) and bulk samples (0.5 mm diameter) are presented in ref [3]. Thus Fe_{66.5}Co₁₀Pr_{3.5}B₂₀ amorphous alloy, cast as ribbon and in bulk form, with the above mentioned dimensions develops a multiphase Fe₃B / α Fe / Nd₂Fe₁₄B structure upon crystallization [3]. In this paper we report the preparation and magnetic properties of (Pr,Dy)_xFe_{70-x}Co₁₀B₂₀ (x = 4,5) bulk nanocomposite permanent magnets. A comparison with thick ribbon counterparts is presented.

2. Experimental

Master alloys were prepared from pure elements and pre-alloyed FeB by arc-melting in an Ar atmosphere. The compositions of the master alloys were: Pr₃Dy₁Fe₆₆Co₁₀B₂₀,

* Corresponding author: marinescu@phys-iasi.ro

$\text{Pr}_{3.5}\text{Dy}_{0.5}\text{Fe}_{66}\text{Co}_{10}\text{B}_{20}$ and $\text{Pr}_4\text{Dy}_1\text{Fe}_{65}\text{Co}_{10}\text{B}_{20}$. Praseodymium has been used instead of neodymium since the intermetallic compound $\text{Pr}_2\text{Fe}_{14}\text{B}$ has a higher anisotropy field as compared to $\text{Nd}_2\text{Fe}_{14}\text{B}$, fact that is important for maintaining a high coercivity in the nanocomposites consisted of hard magnetic and soft magnetic phase. In order to obtain information about the maximum expected thickness of bulk specimens with a fully amorphous structure, as well as to make a general comparison (e.g. heat of crystallization), samples in the form of ribbons were prepared by melt-spinning at chill-roll speeds in the range 5-9 m/s. The maximum thickness of ribbons produced was 350 μm . The preparation procedure for bulk samples was suction casting into a water-cooled copper die maintained at a pressure of $\sim 10^{-2}$ mbar. The as-cast bulk samples were rods of diameter 0.5 mm and tubes of outer diameter 3 mm and wall thicknesses up to 0.3 mm, depending on the mass of the initially molten feedstock, the die cavity diameter, the melt superheat and the flow characteristics of the alloy. The samples structures were examined with an X-Ray Diffractometer (Philips 1050 Diffractometer) and the thermal properties in the as-cast state were investigated using a Differential Scanning Calorimeter (910 DSC Du Pont Instruments) at a heating rate of 40 K/min. The magnetic properties were studied using a Vibrating Sample Magnetometer VSM (Oxford Instruments) with a maximum applied field of 2 T.

3. Results and discussion

Ribbons having an amorphous structure were obtained for thicknesses in the range 130-160 μm and, therefore, it was assumed that bulk rods with diameters as large as 0.5 mm could be obtained by suction die-casting [4]. Thus, a die cavity size of 0.5 mm was employed for casting rods and of 3 mm for casting tubes. The XRD patterns for bulk samples ground to powder are presented in Fig.1 (a). One can note in Fig 1(b) that the amorphous samples reveal a metallic lustre although XRD was necessary to confirm whether the samples were fully or partly amorphous. A fully amorphous structure develops, on controlled crystallization, a uniform nanocrystalline structure. The XRD investigations (using $\text{Co-K}\alpha$ radiation) of the as-cast samples revealed a broad peak or no distinct crystalline diffraction patterns for the rod samples of the $\text{Pr}_3\text{Dy}_1\text{Fe}_{66}\text{Co}_{10}\text{B}_{20}$ and $\text{Pr}_4\text{Dy}_1\text{Fe}_{65}\text{Co}_{10}\text{B}_{20}$ alloys but at least a partly crystalline structure for the tube sample of the $\text{Pr}_{3.5}\text{Dy}_{0.5}\text{Fe}_{66}\text{Co}_{10}\text{B}_{20}$ alloy.

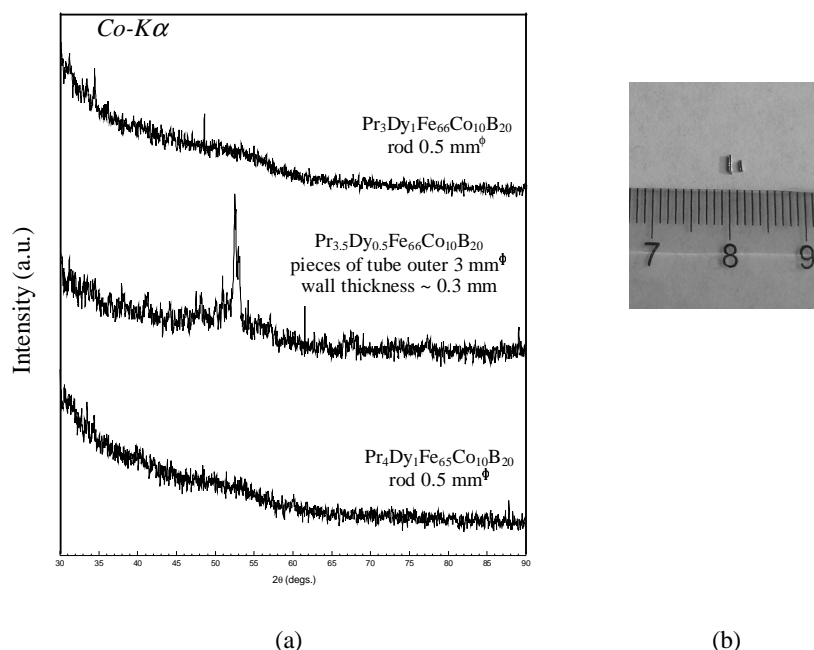


Fig. 1. (a) XRD patterns for as-cast bulk samples of the three alloys; (b) image of rod-shaped $\text{Pr}_3\text{Dy}_1\text{Fe}_{66}\text{Co}_{10}\text{B}_{20}$ samples obtained by suction cast into a die.

DSC curves revealed a two-stage crystallization process in the bulk samples and in the thick ribbons. The total heat of crystallization ΔH_x for specimens of the three alloys are given in Table 1. The values of ΔH_x are larger for ribbons than for bulk samples of the $\text{Pr}_{3.5}\text{Dy}_{0.5}\text{Fe}_{66}\text{Co}_{10}\text{B}_{20}$ and $\text{Pr}_3\text{Dy}_1\text{Fe}_{66}\text{Co}_{10}\text{B}_{20}$ alloys, indicating the existence of crystalline phase in the latter. On the other hand, the value of ΔH_x for the bulk sample of the $\text{Pr}_4\text{Dy}_1\text{Fe}_{65}\text{Co}_{10}\text{B}_{20}$ alloy is larger than for the corresponding fully amorphous ribbon sample and this is ascribed to experimental errors. The crystallization events observed in the DSC traces were used as a basis for choosing the devitrification anneal parameters to induce optimum nanocomposite structures having good hard magnetic properties. The high GFA of this class of alloys is determined by the stoichiometry, including the high metalloids and low rare earth contents, as well as by the addition of solute elements having large atomic size differences from the matrix species and also large negative heats of mixing [5]. Nevertheless, the solute additions must be carefully selected since they can alter the magnetic properties of the subsequently devitrified samples. The addition of Co is known to increase the Curie temperature by partial substitution for the Fe in the 2:14:1 phase unit cell and small substitutions of Dy increase the anisotropy field of the 2:14:1 phase and thus the coercivity [6].

Table 1. Heat of crystallization determined from DSC on $(\text{Pr,Dy})_x\text{Fe}_{70-x}\text{Co}_{10}\text{B}_{20}$ ($x=4,5$) as cast alloys.

Alloy composition / max. thickness	Heat of crystallization	Alloy composition / sample type	Heat of crystallization
$\text{Pr}_{3.5}\text{Dy}_{0.5}\text{Fe}_{66}\text{Co}_{10}\text{B}_{20}$ $t_{\text{max}}=130\mu\text{m}$	81.9J/g	$\text{Pr}_{3.5}\text{Dy}_{0.5}\text{Fe}_{66}\text{Co}_{10}\text{B}_{20}$ tube pieces	24.6J/g
$\text{Pr}_3\text{Dy}_1\text{Fe}_{66}\text{Co}_{10}\text{B}_{20}$ $t_{\text{max}}=150\mu\text{m}$	85.4J/g	$\text{Pr}_3\text{Dy}_1\text{Fe}_{66}\text{Co}_{10}\text{B}_{20}$ tube pieces	66.3J/g
$\text{Pr}_4\text{Dy}_1\text{Fe}_{65}\text{Co}_{10}\text{B}_{20}$ $t_{\text{max}}=160\mu\text{m}$	70.9J/g	$\text{Pr}_4\text{Dy}_1\text{Fe}_{65}\text{Co}_{10}\text{B}_{20}$ tube pieces	77.3J/g

The as-cast $(\text{Pr,Dy})_x\text{Fe}_{70-x}\text{Co}_{10}\text{B}_{20}$ ($x = 4,5$) samples are magnetically soft and the magnetic hardness develops as the samples are devitrified to the optimum nanostructure. The XRD investigations on annealed samples (patterns are not given here) reveal a multi-phase 2:14:1 / α -Fe, Fe_3B nanostructure. Fig. 2 presents the hysteresis loops for bulk samples annealed under various conditions. The best magnetic properties were achieved for the $\text{Pr}_3\text{Dy}_1\text{Fe}_{66}\text{Co}_{10}\text{B}_{20}$ rod and tube samples heat treated at 670°C for 10 min.; these were: $iH_c = 287$ kA/m, $\mu_0M_r = 0.92$ T, $(\text{BH})_{\text{max}} = 58$ kJ/m³ and $iH_c = 293$ kA/m, $\mu_0M_r = 1.0$ T, $(\text{BH})_{\text{max}} = 66$ kJ/m³, respectively. Table 2 compares the best magnetic properties achieved for the bulk and ribbon samples of each alloy.

One can note that the thick ribbons generally have better property combinations than the corresponding bulk samples. For instance, for the $\text{Pr}_{3.5}\text{Dy}_{0.5}\text{Fe}_{66}\text{Co}_{10}\text{B}_{20}$ alloy, $\mu_0M_r = 1.45$ T, $iH_c = 247$ kA/m and $(\text{BH})_{\text{max}} = 106$ kJ/m³. However, the highest coercivity from among all the samples (293 kA/m) was achieved for a $\text{Pr}_3\text{Dy}_1\text{Fe}_{66}\text{Co}_{10}\text{B}_{20}$ tube sample annealed at 670°C for 10 min.

The good permanent magnetic properties in nanocomposite systems that contain soft and hard magnetic phases are determined by the exchange coupling effect responsible for soft grain hardening. From the measurement of irreversible susceptibility (first derivative of the irreversible magnetization with field) as a function of the applied field, one can deduce, associated with its maximum, the nucleation field H_n for domain reversal within the hard magnetic phase. Starting with this value of the applied field, irreversible demagnetisation processes occur. The exchange coupling is effective when the nucleation field equals the coercive field. From our magnetic studies (Fig. 3), we observe that the nucleation field H_n for domain reversal in bulk nanocomposite $(\text{Pr,Dy})_x\text{Fe}_{70-x}\text{Co}_{10}\text{B}_{20}$ ($x = 4,5$) magnets exceeds iH_c , whereas, in optimally annealed $\text{Pr}_{3.5}\text{Dy}_{0.5}\text{Fe}_{66}\text{Co}_{10}\text{B}_{20}$ ribbons (630°C for 15 min), H_n is slightly lower than iH_c . A nucleation field that is larger than the coercive field suggests that the grain size of the soft phase exceeds double the

domain wall width of the 2:14:1 hard phase [1] and thus that the soft phase grains are not completely exchange coupled.

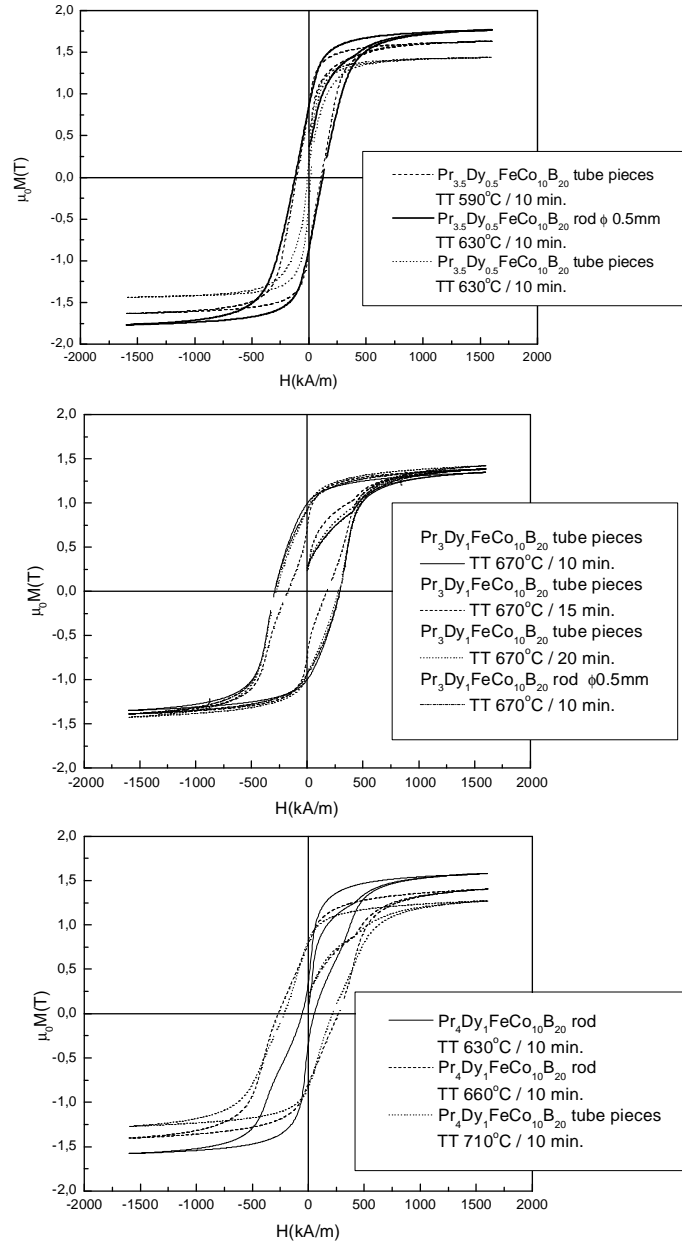


Fig. 2. Hysteresis loops for devitrification-annealed $(\text{Pr,Dy})_x\text{Fe}_{70-x}\text{Co}_{10}\text{B}_{20}$ ($x=4,5$) bulk samples.

Table 2. The magnetic properties for bulk samples compared to ribbon samples.

Alloy composition	Sample type / Annealing parameters	iH_c [kA/m]	$\mu_0 M_r$ [T]	$(BH)_{\max}$ [kJ/m ³]
$\text{Pr}_3\text{Dy}_1\text{Fe}_{66}\text{Co}_{10}\text{B}_{20}$	Tube: 670°C/10min	293	1.0	66
	Rod: 670°C/10min	287	0.92	58
	Ribbons $-t_{\max}=150\mu\text{m}$: 660°C/10min	284	1.09	87
$\text{Pr}_{3.5}\text{Dy}_{0.5}\text{Fe}_{61}\text{Co}_{10}\text{B}_{20}$	Rod: 630°C/10min	120	0.86	21
	Ribbons $-t_{\max}=130\mu\text{m}$: 630°C/15min	247	1.45	106
$\text{Pr}_4\text{Dy}_1\text{Fe}_{65}\text{Co}_{10}\text{B}_{20}$	Rod: 660°C/10min	263	0.77	36
	Ribbons $-t_{\max}=160\mu\text{m}$: 630°C/10min	279	1.0	57

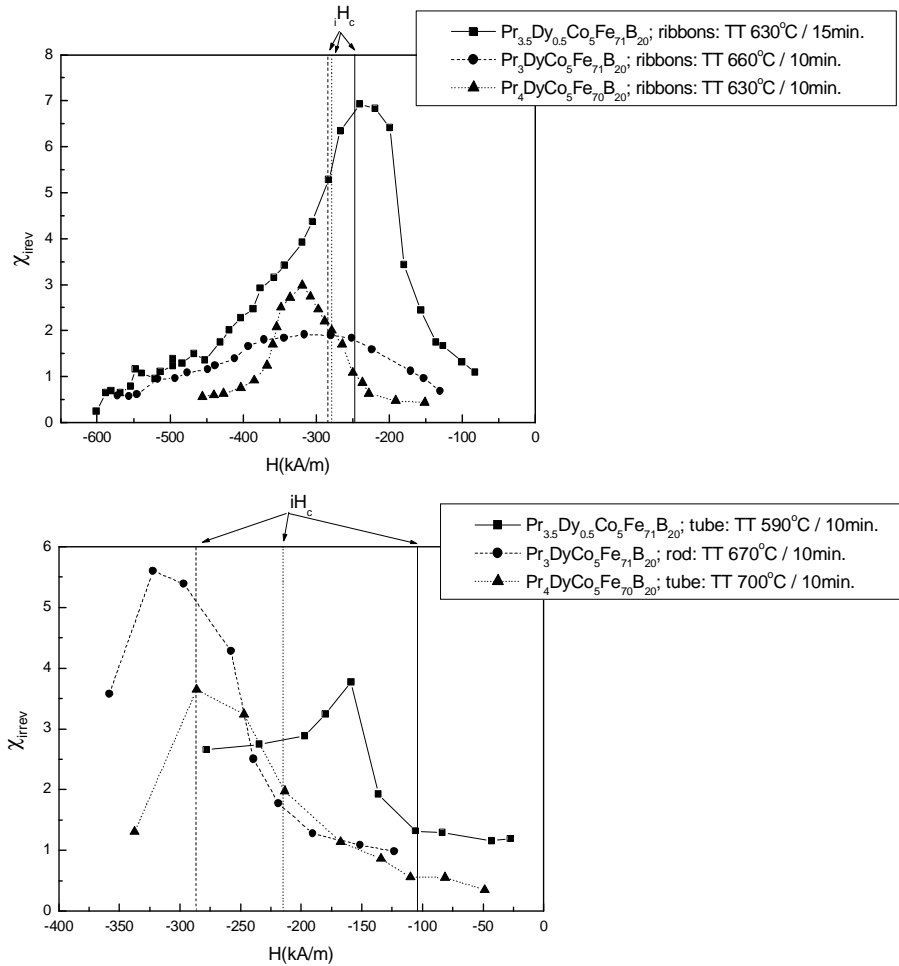


Fig. 3. Irreversible susceptibility as a function of the applied field for nanocomposite thick ribbon and bulk samples of $(\text{Pr,Dy})_x\text{Fe}_{70-x}\text{Co}_{10}\text{B}_{20}$ ($x = 4,5$) alloys.

5. Conclusions

Bulk amorphous samples, in the form of rods of diameter 0.5 mm and tubes with outer diameters of 3mm and wall thicknesses up to 0.3 mm, having compositions $\text{Pr}_3\text{Dy}_1\text{Fe}_{66}\text{Co}_{10}\text{B}_{20}$, $\text{Pr}_{3.5}\text{Dy}_{0.5}\text{Fe}_{66}\text{Co}_{10}\text{B}_{20}$ and $\text{Pr}_4\text{Dy}_1\text{Fe}_{65}\text{Co}_{10}\text{B}_{20}$ were prepared by suction die casting. Amorphous samples in the form of thick ribbons (with thicknesses in the range 130-160 μm) were prepared by melt spinning for comparison. The devitrified bulk samples with optimum nanocomposite 2:14:1 / α -Fe, Fe_3B structures has good hard magnetic properties, with values of remanent magnetization as high as $\mu_0 M_r = 1.0$ T and maximum coercivity iH_c up to 293 kA/m. The remanence of the nanocomposite bulk samples is lower than that obtained for the corresponding thick ribbon sample for each composition, whereas iH_c is larger. The nucleation field H_n for reverse domains in the bulk nanocomposite magnets exceeds iH_c , suggesting that the exchange coupling between the hard and soft phase grains is not fully effective due to insufficiently fine soft grains. In contrast, for optimally annealed thick ribbons, H_n is slightly smaller than iH_c , suggesting that the soft phase grains are completely coupled to neighbouring hard grains.

Acknowledgement

The research at Sheffield was performed under European RTN Network “*Bulk Metallic Glasses*”: HRPN-CT-2000-0033.

References

- [1] E. F. Kneller, R. Hawig, IEEE Trans. Magn. **MAG-27**, 3588 (1991).
- [2] P. C. Pawlik, H. A. Davies, Scripta Mater. **49**, 755 (2003).
- [3] W. Zhang, A. Inoue, J. Appl. Phys. **91**, 8834 (2002).
- [4] P. Pawlik, H. A. Davies, M. R. J. Gibbs, Appl. Phys. Lett. **83**, 2775 (2003).
- [5] A. Inoue, Bulk Amorphous Alloys – Preparation and Fundamental Characteristics, Materials Science Foundation, vol. 4, 1998.
- [6] G. C. Hadjipanayis, in: Rare Earth-Iron Permanent Magnets, Edited by J.M.D. Coey, Clarendon, Oxford, 1996.